An artificial neural network approach for the control of the laser milling process

Article *in* The International Journal of Advanced Manufacturing Technology · June 2012

DOI: 10.1007/s00170-012-4457-9

CITATIONS
39

READS
250

4 authors, including:

G. Casalino
Politecnico di Bari
125 PUBLICATIONS **2,404** CITATIONS
SEE PROFILE

Cesare Bonserio
Politecnico di Bari
5 PUBLICATIONS **147** CITATIONS
SEE PROFILE

Int J Adv Manuf Technol (2013) 66:1777–1784
DOI 10.1007/s00170-012-4457-9

ORIGINAL ARTICLE

An artificial neural network approach for the control of the laser milling process

S. L. Campanelli · G. Casalino · A. D. Ludovico · C. Bonserio

Received: 21 September 2010 / Accepted: 6 August 2012 / Published online: 8 September 2012

Abstract Laser milling (LM) can be classified as a layer manufacturing process in which the material is removed by a laser beam by means of the ablation mechanism. It is a laser machining process which uses a laser beam to produce 3D shapes into a wide variety of materials. It is also known as laser ablation. It shows clear advantages versus the traditional milling such as the unlimited choice of materials, the direct use of computer-aided design structure data, the high geometric flexibility, and the touchless tool. LM requires the selection of optimal machining parameters for the job. Unlike the mechanical milling and the mechanical incision, the depth of the single removed layer is chosen at the beginning as input parameter of the process. In LM, the ablated depth depends from the process parameters such as laser power, scan speed, pulse duration, and pulse frequency. This work aims to develop an algorithm that can predict the parameters necessary to execute the material removal with a preset ablation depth. Using the results of an experimental campaign, the laser milling process was modeled by means of a back-propagation artificial neural network. Then, an iterative algorithm, based on the previous trained neural network, permitted to calculate the scanning velocity and pulse frequency that approached for the best the preset ablation depth. The developed approach represents a mean for the rational selection of laser ablation process parameters. It can be performed in an intuitive manner since it uses simple artificial intelligence like the artificial neural network.

Keywords Laser milling · ANN modeling · Ablation depth · Velocity and pulse frequency optimization

Abbreviations

P %	Peak power
F_p	Pulse frequency
v	Scan speed
H_d	Hatch distance
Δz	Depth of removed material
Δz_n	Depth value measured after n ablated layers
LMA	Levenberg–Marquardt back-propagation algorithm
J	Jacobian matrix
e	Network error
μ	Scalar in the approximation to the Hessian matrix
(Δz_t)	Preselected ablation depth (target)
(Δz_s)	Simulated ablation depth
$(E\ \%)_{\max}$	Preselected max error for parameters optimization
E %	Error for parameters optimization
$(F_p)_{i+1}$	Pulse frequency at i+1 step
v_{i+1}	Velocity at i+1 step

1 Introduction

Laser milling (LM) is a growing technology in the field of micromanufacturing processes thanks to the ability to produce extremely fine and accurate 3D objects in a wide range of materials. In LM technology, the material is removed by a laser beam through the layer by layer ablation mechanism. The process consists in an ablation operation in which the material is removed during the action of a laser pulse, which melts the material and heats it up to the vaporization temperature.

S. L. Campanelli (✉) · G. Casalino · A. D. Ludovico
Department of Mechanics, Mathematics and Management,
Politecnico di Bari,
Viale Japigia 182,
Bari, Italy
e-mail: campanel@poliba.it

C. Bonserio
Centro Laser,
Valenzano, Bari, Italy

The success of laser milling as a micromachining process is due to the integration between the laser ablation mechanism and the Computer Numerical Control (CNC) program, which is generated directly from computer-aided design (CAD) data. LM shows clear advantages compared to the traditional manufacturing processes: the capability to machine difficult-to-machine materials such as ceramics, graphite, and cemented carbides and the totally absence of tool wear because of the touchless tool, surface finish, aspect ratio, dimensional accuracy, and minimum feature size [1, 2]. Moreover, LM is a process well suited to machining of very finely detailed cavities or microfluidic channels.

Since 2001, Heyl et al. [3] demonstrated that laser ablation leads to equivalent surface qualities for manufacturing of microembossing tools at a higher speed and with more geometrical flexibility compared to the traditional high-end electrical discharge milling procedures. Riccardi et al. [4] described the fabrication of high-resolution bubble ink jet nozzle having 55-μm diameters on a thickness of 50 μm of polyimide. Windholz [5] described micromachining of diamond by means of a microsecond pulse Nd:YAG and nanosecond pulse excimer lasers; Kovalenko [6] reported microdrilling, microcutting, and micromilling of semiconductors with green laser.

Karnakis et al. (2006) showed that both nano- and picosecond lasers can be used for high-quality laser micromilling of materials such as ceramics, dielectrics, and metals difficult to machine with ultrahigh precision otherwise using conventional methods [7]. The value of the depth of removed material determines the accuracy of parts produced through a layer manufacturing technology. Unlike the traditional technologies, as mechanical milling, mechanical incision, etc., in which the depth of the single removed layer is chosen at the beginning as input parameter of the process, in LM, the ablated depth depends from the process parameters such as laser power, scan velocity, hatch distance, and pulse frequency.

Although a good number of fundamental research have already been done on laser ablation, further research is still needed for optimal control of machining parameters. Kaldos et al. [8] presented an investigation to determine the process window by using laser ablation for several materials, which allows for the finding of optimum process parameters for the maximum removal rate. Campanelli et al. [9, 10] studied the influence of process parameters on quality of built parts, finding the optimal set up to obtain maximization of ablation depth and, at the same time, low surface roughness. Mannio et al. studied the ablation thresholds in ultrafast laser micromachining of common metals in air [11].

From this number of papers, the sensitiveness of the laser ablation to the process parameters has been pointed. Therefore, the aim of this paper was to implement an Artificial Neural Network (ANN) to model the LM process in order to produce an intelligent algorithm that would be able to predict the most appropriate parameters setting to use with a given ablation depth.

ANNs come in the statistical or evidence-based artificial intelligence. Statistical or evidence-based artificial intelligence use optimization techniques to automatically improve the performance of a piece of software, based on evidence present in measurement data. An ANN is a parallel system capable of resolving paradigms that linear computing cannot.

Over the years, they have given various solutions to the engineering problems of modeling and optimization [12]. Among the numerous applications available, it is worth to highlight some works in the field of laser manufacturing. Some authors promoted their use in the filed of laser welding. Olabi et al. applied the statistical approach to the mechanical and microstructural characterization of steel weld [13, 14]. Casalino et al. investigated the weldability and weld soundness of light metal alloys [15]. Basem et al. used multilayered neural network to model the nonlinear laser micromachining process [16]. Luo et al. diagnosed weld failure due to laser welding [17]. Some authors performed very interesting investigation using two or more different artificial intelligence. Just to limit to the filed of laser welding, they are worth to remember Casalino and Minutolo who proposed a model for evaluation of laser welding efficiency and quality using an artificial neural network and fuzzy logic [18] and Park and Rhee who resolved a problem of optimization using neural network and genetic algorithms for aluminum laser welding automation [19].

Because of the elevate number of process parameters involved in the process and in order to reduce the number of tests necessary to train the neural network, a preliminary experimental investigation was performed. It allowed, also, evaluating the influence of the main parameters involved in the LM process on the success of the ablation process in terms of depth of removed material. Later on it, the developed ANN model was able to determine values of the scan speed and of the pulse frequency, corresponding to an established depth of removed material, optimizing the process productivity.

2 Experimental procedure

2.1 Laser milling equipment and materials

CNC programs for LM are obtained directly from a 3D model of the workpiece. Figure 1b shows a complex sample obtained by laser milling starting from CAD data (Fig. 1a). In ablation processes, several parameters can be controlled and varied in order to get complex parts with optimized quality.

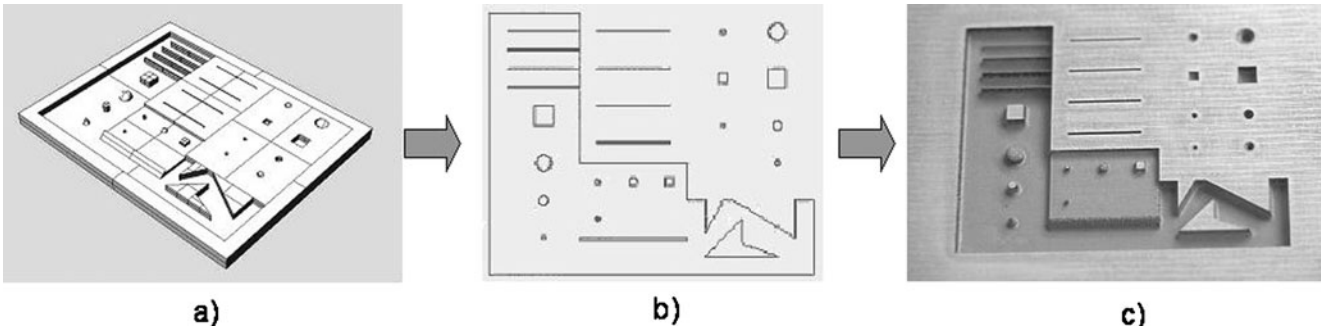

Fig. 1 Example of manufacturing a complex feature by laser milling: (**a**) 3D CAD file, (**b**) slicing operation, and (**c**) final object

Previous works [20, 21] showed that the main parameters, affecting the ablated depth, are peak power (P %), pulse frequency (F_p), scan speed (v), and hatch distance (H_d), where:

- P is the laser's instantaneous output power during the laser pulse;
- F_p pulse frequency or repetition rate is the number of pulses per second from the laser, measured in Hertz;
- v is the velocity by which the laser beam moves over the material surface; and
- H_d, as illustrated in Fig. 2, is defined as the distance between two consecutive spot diameters, and it is related to F_p and v by the following equation:

$$H_d = \frac{v}{F_p}. \tag{1}$$

The machine used in this research work was equipped with an Nd:YVO_4 laser source (wave length 1,064 nm) with a maximum peak power of 40 kW. The major parameters of the machine are shown in Table 1.

Nd:YVO_4 is a solid state laser having ions of neodymium introduced as impurities in crystals of YVO4 [22]. The lasers of this type have begun in the last times to replace Nd:YAG lasers in several applications such as spectroscopy, medical diagnoses, and laser surface processes. In comparison to Nd:YAG laser, Nd:YVO4 presents some advantages: the ability to produce more compact systems thanks to a greater coefficient of absorption, a bigger efficiency due to the elevated spectrum of absorption at the wavelength to which the pumping happens. Plates of the aluminum–magnesium alloy 5754 were used for all experimental tests. Table 2 shows the chemical composition of this material.

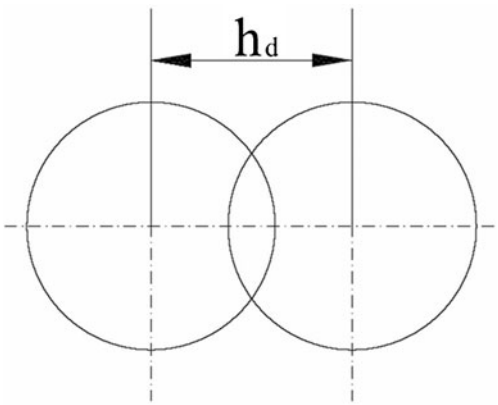

Fig. 2 Two consecutive laser pulses

2.2 Preliminary screening of the most affecting parameters

A 2^3 full factorial design was planned for the simultaneous study of the effects of the main parameters on the success of the ablation process in terms of depth of removed material (Δz). This study was used, also, as screening to reduce the number of factors for the neural network modeling of the process.

The three parameters P %, F_p, and H_d were chosen for this purpose. These parameters were changed on two different levels, respectively, the minimum and the maximum value of the possible variability range, as illustrated in Table 3, resulting in eight combinations. In order to have meaningful results, three identical tests were performed for each combination, which resulted in a total of 24 parts. Moreover, because of the difficulty to measure a too small value of Δz, every square chosen for tests was marked nine

Table 1 Specification details of laser machine

Specification	Description
Laser type	Nd:YVO4
Wavelength (nm)	1,064
Operation mode	Q-switched (pulsed)
Scan speed (mm/s)	0/2,000
Average power (W)	30
Peak power (kW)	10/40
Pulse frequency (kHz)	1/100
Pulse width (nm)	5
Focus diameter (μm)	40

Table 2 Chemical composition of the aluminum alloy 5754

	Si	Fe	Mn	Mg	Al
Al 5754	0.1	0.31	0.34	2.87	Balance

times. The value of Δz related to the single layer was obtained through the Eq. 2, in which n is the number of ablated layers (nine in this case), and Δz_n is the depth value measured after n ablated layers.

$$\Delta z = \frac{\Delta z_n}{n} \tag{2}$$

Figure 3 shows the main effects plot for Δz versus P %, F_p, and H_d. It can be observed that:

- The mean value of Δz is maximum for P % set to the maximum value 100 %, and it is minimum for P % set to the minimum value 30 %;
- The mean value of Δz is maximum for F_p set to the minimum value 10 kHz and, it is minimum for F_p set to the maximum value 100 kHz;
- The mean value of Δz is maximum for H_d set to the minimum value 5 μm and, it is minimum for H_d set to the maximum value 20 μm;
- Comparing the slope of the lines, it results that the magnitude of the effect for P % is greater than for F_p and H_d; P % is the most affecting parameter on Δz. Consequently, in order to maximize the ablation depth Δz, it is necessary to set P % to 100 %.

For instance, next experiments on neural network have been conducted considering only the variability of the two parameters F_p and H_d, setting P % to the maximum value 100 %. Moreover, because of the necessity to control both the ablation depth and the velocity of the process, the scan speed v was considered on behalf of H_d, considering that the three parameters v, H_d, and F_p are related to each other by means of the Eq. 1. Consequently, the ablation depth was controlled changing F_p and v.

Table 3 Machining parameters

Machining parameters	Levels	
	L1	L2
Peak power (%)	30	100
Pulse frequency (kHz)	10	90
Hatch distance (μm)	5	20

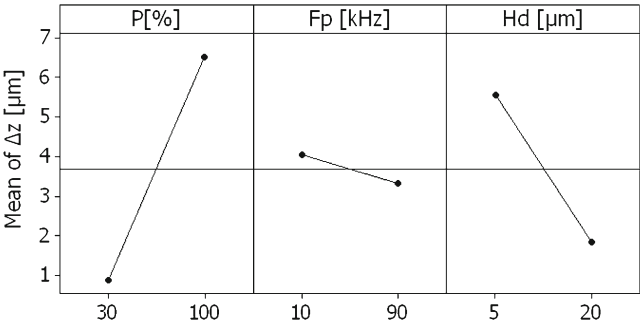

Fig. 3 Main effects plot for Δz versus P %, F_p, and H_d

2.3 Experimental tests for ANN

In this step, an artificial neural network was implemented to model the relationship between the depth of ablated material Δz and the two input process parameters F_p and v. A set of 70 specimens were produced, varying the two input process parameters F_p and v, respectively, in the range 10–100 kHz and 50–2,000 mm/s.

The value of Δz was calculated again with Eq. 2, considering the ablation of nine layers (n=9). Finally, the ablated depth Δz was measured by means of an optical microscope.

3 LM modelling by Artificial Neural Network

3.1 Presentation of the ANN

Seventy couples of input–output patterns were collected for the construction of the artificial neural network. The architecture of the ANN was characterized from a different couple of input–output pattern. The input pattern was composed, according to Eq. 3, by two parameters x_1 and x_2:

$$x = \begin{bmatrix} x_1 \\ x_2 \end{bmatrix} \tag{3}$$

where $x_1 = F_p$ and $x_2 = v$. The output pattern was composed by only one element corresponding to ablation depth Δz, according to Eq. 4:

$$y = [\Delta z]. \tag{4}$$

Each model was trained to learn relationships between input patterns and output element, so that each model had only one output channel as showed in Fig. 4. Feed-forward-three-layer neural networks have been applied in this work, and the Levenberg–Marquardt backpropagation algorithm (LMA) was employed to train them. Out of the entire training algorithm, the LMA is

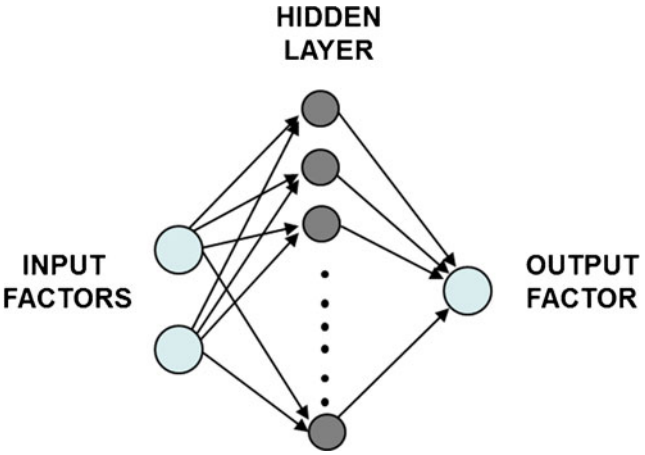

Fig. 4 Configuration of the neural network

the fastest and the least memory consuming one [23]. The classical back-propagation training algorithms, based on gradient descent or on gradient descent with momentum, are often too slow for practical problems. The Levenberg–Marquardt back-propagation algorithm allows a convergence from ten to 100 times faster than the above algorithms. This algorithm appears to be the fastest method for training moderate-sized feed-forward neural networks.

The LMA was designed to approach second-order training speed without having to compute the Hessian matrix. When the performance function has the form of a sum of squares, as in training feed-forward networks, then the Levenberg–Marquardt algorithm uses an approximation to the Hessian matrix in the following Newton-like update:

$$x_{k+1} = x_k \mathrm{J}^{\mathrm{T}}[\mathrm{J} + \mu \mathrm{I}]^{-1} \mathrm{J}^{\mathrm{T}} \mathrm{e} \quad (5)$$

where the Jacobian matrix "J" contains first derivatives of the network errors with respect to the weights and biases, and "e" is a vector of network errors.

During the calculation, μ is decreased after each successful step (reduction in performance function) and is increased only when a tentative step would increase the performance function. In this way, the performance function will always be reduced at each iteration of the algorithm.

3.2 Setting and training

It is a well-known fact that the performance of an ANN is strongly influenced by the training patterns choice and by the hidden layer neuron number. The training dataset should be as more process representative as possible, and this could be a problem, particularly when the available dataset is limited despite the complexity and nonlinearity of the input–output connections. In fact, a certain fraction of the collected data have to be used for the testing phase both to avoid "overtraining" and to evaluate the final performance of the trained network. The testing dataset should be, at the same time, large enough to make testing reliable and small enough to assure a representative training dataset.

In addition, given the test data fraction, the choice of the particular test patterns among the global dataset plays an important role in the quality of the final ANN model because it determines the representativeness of both the test and training data. For what concern the hidden neurons number, it should not be too small so to assure a good training performance (low training error), but it should not be too large in order to avoid overtraining (low test error).

The developed algorithm is based on a large number of training iteration with the variation of three fundamental parameters: the test data fraction, the extracted test patterns, and the number of hidden neurons. Specifically, the test data fraction was changed on three levels (15, 25, and 50 %); a random extraction was chosen for test data patterns, and finally, the number of hidden neurons was changed on five levels (3, 5, 10, 20, and 30).

The range of the last parameters, as well as the remaining training parameters (training functions, learning rate, epochs, etc.), are suitably chosen by the user. For each training process, a continuous control on the difference between training and test error is conducted, stopping the process if negative values are detected in order to avoid overtraining.

The most performing network is finally determined on the bases of three performance indices: the mean training relative error, the mean test relative error, and the standard deviation of the last. The fundamental characteristics of the ANN obtained with those values consist of 32 neurons for the hidden layer and with 25 % test data fraction.

In this training protocol, the used parameter values were: epochs=50, learning rate=0.001, ratio to increase learning rate=0.1, and ratio to decrease learning rate=10. The obtained average training error was 3.20 %; the average test error, 5.69 %.

4 Automatic optimization of the working parameters

After the ANN network was built, a trial-and-error algorithm was implemented in order to select the optimum levels of the working input for the available laser, i.e., speed (v) and pulse frequency (F_p), for a preselected ablation depth (Δz_t). The optimization had the purpose to improve the speed of the process; thus, the maximum values of the parameter v were searched for each values of (Δz_t). The model works by searching convergence to a preset value. The preset value is the error E % that was calculated by means of the Eq. 6,

for this purpose.

$$E\,\% = \frac{|\Delta z_t - \Delta z_s|}{\Delta z_t}.100 \quad (6)$$

As the first step of the algorithm, the speed and frequency were set to the highest available levels, which were 2,000 mm/s and 100 kHz, respectively. Then, the ablation depth for maximum input levels (Δz_s) was calculated and compared with the preselected one on the basis on a preselected maximum error ($E\,\%_{max}$)

The stopping criterion is as follow: in the case $E\,\% < E\,\%_{max}$, the couple of the input parameters that would produce Δz_s have to be set to the maximum process speed and frequency, which were $v = v_{max}$ and $F_p = F_{pmax}$. Indeed, in the case $E\,\% > E\,\%_{max}$, the optimization process began to reduce pulse frequency by means of the relation $(F_p)_{i+1} = (F_i - \Delta F_{i+1})$ with $\Delta F_{i+1}=1$ and leaving v to the maximum value in order to calculate a new Δz_s, by which a new evaluation error $E\,\%$ had to be calculated. The pulse frequency reduction process was allowed till $F_p = F_{pmin}$, where F_{pmin} was

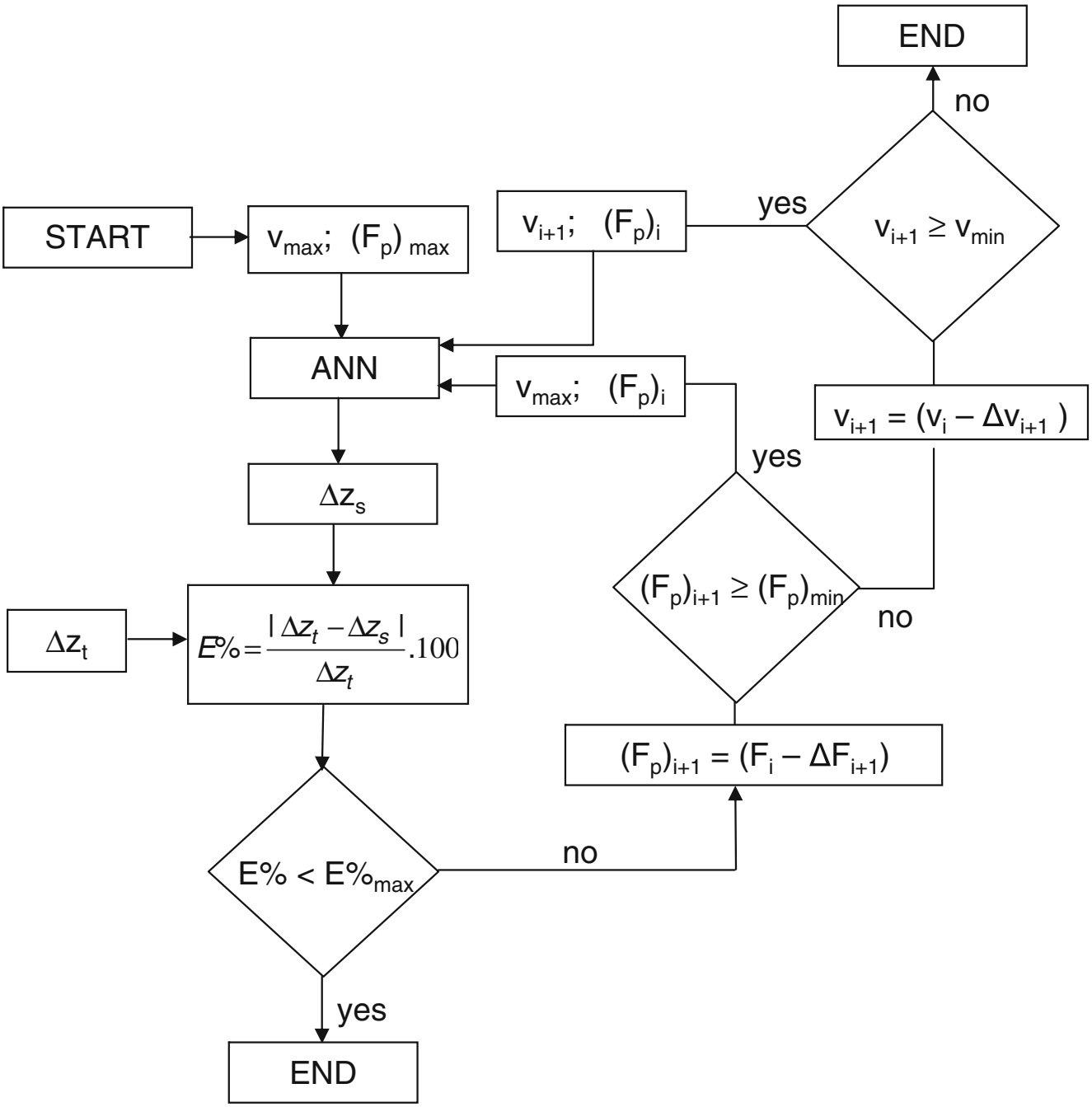

Fig. 5 Flow chart of the optimal algorithm through ANN model

the minimum value of the considered range. In case $F_p = F_{p\min}$ and still is $E\ \% < E\ \%_{\max}$, the algorithm began to reduce speed by means of the relation $v_{i+1} = (v_i - \Delta v_{i+1})$ with $\Delta v_{i+1}=1$.

The calculation loop was repeated for every new speed value. The optimization process stopped when the condition $E\ \% < E\ \%_{\max}$ was obtained, or minimum values for speed and frequency were reached.

Figure 5 shows the flow chart of the pattern followed from the input of the initial speed and frequency to the optimum ones. Figure 6 shows the E % score with Δz_t. The maximum E % is always lower than 5 % for values of Δz_t available with a single ablated layer.

5 Discussion

In the range of investigation, ANN predictive models are effective algorithms that predict the process outputs for the specific materials. Furthermore, the model can be used to select the input for a required process output that is within the range of the original input data used during the training phase.

In this work, a feed-forward three-layer, LMA back-propagation ANN was used to construct a LM model to predict the response parameter (ablation depth) as a function of two different control parameters (v and F_p). The predicted values can be used for the optimization goal. In fact, the trial and error algorithm, which was used to calculate the optimal couple of process parameters v and F_p, corresponded to an established value of ablation depth (Δz_t). The optimization goal was to choose the maximum possible speed v in the entire available set.

Results of the algorithm are plotted in Figs. 7 and 8. Specifically, Fig. 7 displays values of the scan speed v corresponding to a certain value of ablation depth (Δz_t). It can be observed that v decreases with the increase of Δz_t. Lower ablation depths (<2.5 μm) can be obtained with velocities near the maximum considered value of 2,000 mm/s. Higher ablation depths (>10 μm) can be achieved for values of scan speed between 460 and 510 mm/s. Figure 8 shows values of pulse frequency F_p versus Δz_t. Lower and higher values of ablation depths can be reached for F_p close by the maximum value in the investigated range (100 kHz); medium values (between 2.5 and 10 μm) were related to 80 to 100 kHz.

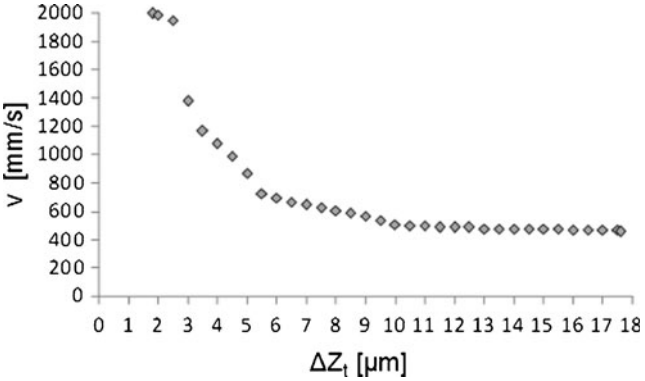

Fig. 7 Values of the maximum scan speed corresponding to an established ablation depth Δz_t

The most important disadvantage of the proposed method is that the experimental knowledge, which is fundamental to the reliability and sensitiveness of the control of the process, can be expensive in terms of money and time. Major advantages of this approach are that a rational selection of laser ablation process parameters can be performed in an intuitive manner since it uses simple calculation. Indeed, the plots in Figs. 6, 7 and 8 permit a rapid evaluation of the sensitiveness of the calculated ablation depth versus the desired depth and the related v and F_p.

Moreover, ANN models can be used to calculate ablation depths that were not measured during the experimental work. The employment of an optimization technique based on the ANN models allows the selection of the process control parameter for achieving a target response, which

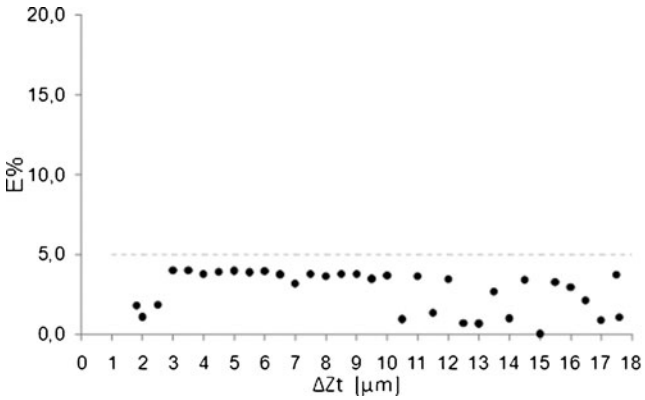

Fig. 6 E % of simulated response versus target response referred to best speed parameters

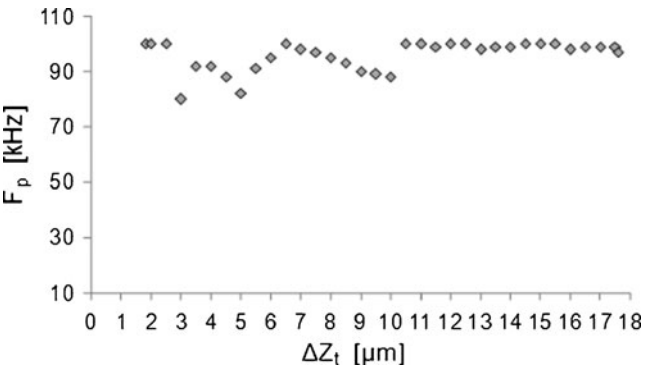

Fig. 8 Values of pulse frequency to use in combination with the maximum speeds for an established ablation depth Δz_t

increases the process performance and improves the final product quality.

6 Conclusion and future directions

Unlike the traditional technologies, as mechanical milling, mechanical incision, etc., in which the depth of the single removed layer is chosen at the beginning as input parameter of the process, in laser milling, the ablation depth Δz depends on the process parameters such as laser power, scan velocity, hatch distance, and pulse frequency. In this paper, on the basis of a statistical investigation on the effects of the main process parameters on the ablation depth Δz, an artificial neural network was implemented to select the velocity and pulse frequency in order to control Δz.

That goal was achieved by a recurrent automatic algorithm that encapsulated the above-mentioned ANN. It was found that the artificial neural network, together with the proposed optimization algorithm, allows simulating the laser milling process with the maximum process speed, with an actual error lower than 5 %. Through this optimization strategy, it was possible to obtain optimal parametric combinations, which will lead to efficient utilization of laser milling in practice.

This here-presented approach to laser milling control could be improved considering one more response parameter, i.e., the surface roughness, in addition to ablation depth. In that case, the statistical approach will permit to investigate also the interactions between the process parameters, and the ANN will be trained and validated with a two neurons output layer, which can improve significantly the quality of laser-milled parts. In that context, other meta-heuristic techniques and other evolutionary swarm intelligence algorithms could be tested and compared with the result obtained in this work.

References

1. Pham DT, Dimov SS, Petkov PV, Dobrev T (2005) Laser milling for micro-tooling. CU IMRC Working Paper Series, Cardiff University, UK
2. Pham DT, Dimov SS, Ji C, Petkov PV, Dobrev T (2004) Laser milling as a "rapid" micromanufacturing process. Proc Inst Mech Eng J Eng Manuf 218(Part B):1–7
3. Heyl P, Olschewski T, Wijnaendts RW (2001) Manufacturing of 3D structures for micro-tools using laser ablation. Microelectron Eng 57(58):775–780
4. Riccardi G, Cantello M, Mariotti F, Giacosa P (1998) Micromachining with excimer laser. CIRP Ann 47(1):145–148
5. Windholz R, Molian P (1997) Nanosecond pulsed excimer laser machining of CVD diamond and HOPG graphite. J Mater Sci 32:4295–4301
6. Kovalenko V, Anyakin M, Uno Y (2000) Modelling and optimisation of laser semiconductor cutting. Proc ICALEO Laser Micro-Fabr 90:D82–D92
7. Karnakis D, Rutterford G, Knowles M, Dobrev T, Petkov P, Dimov S (2006) High quality laser milling of ceramics, dielectrics and metals using nanosecond and picosecond lasers. SPIE Photonics West LASE 2006, San Jose CA, USA, 6106
8. Kaldos A, Pieper HJ, Wolfb E, Krause M (2004) Laser machining in die making—a modern rapid tooling process. J Mater Process Technol 155(156):1815–1820
9. Campanelli SL, Ludovico AD, Bonserio C, Cavalluzzi P, Cinquepalmi M (2007) Experimental analysis of the laser milling process parameters. J Mater Process Technol 191:220–223
10. Campanelli SL, Ludovico AD, Deramo C (2007) Dimensional accuracy optimisation of the laser milling process. Proceedings of the 26 International Congress on Applications of Lasers and Electro–Optics (ICALEO), Orlando, Florida
11. Mannio P, Magee J, Coyne E, O'Connor GM (2003) Ablation thresholds in ultrafast laser micro-machining of common metals in air. Proc SPIE 4876:470–478
12. Ganesan T, Vasant P, Irraivan E (2011) Solving engineering optimization problems with KKT Hopfield neural networks. Int Rev Mech Eng 7(7):1333–1339
13. Olabi AG, Casalino G, Benyounis KY, Rotondo A (2007) Minimisation of the residual stress in the heat affected zone by means of numerical methods. Mater Des 28(8):2295–2302
14. Olabi AG, Casalino G, Benyounis KY, Hashmi MSJ (2006) An ANN and Taguchi algorithms integrated approach to the optimization of CO_2 laser welding. Adv Eng Softw 37(10):643–648
15. Casalino G, Curcio F, Minutolo FMC (2005) Investigation on Ti6Al4V laser welding using statistical and Taguchi approaches. J Mater Process Technol 167(2–3):422–428
16. Yousef BF, Knopf GK, Bordatchev EV, Nikumb SK (2003) Neural network modeling and analysis of the material removal process during laser machining. Int J Adv Manuf Technol 22(1–2):41–53
17. Luo H, Zeng H, Hu L, Hu X, Zhou Z (2005) Application of artificial neural network in laser welding defect diagnosis. J Mater Process Technol 170(1–2):403–411
18. Casalino G, Minutolo FMC (2004) A model for evaluation of laser welding efficiency and quality using an artificial neural network and fuzzy logic. Proc Inst Mech Eng B J Eng Manuf 218(6):641–646
19. Park YW, Rhee S (2008) Process modeling and parameter optimization using neural network and genetic algorithms for aluminum laser welding automation. Int J Adv Manuf Technol 37 (9–10):1014–1021
20. Kuhl M (2002) From macro to micro—the development of laser ablation. Proceedings of ICALEO 2002
21. Tsai CH, Chen HW (2003) Laser milling of cavity in ceramic substrate by fracture-machining element technique. J Mater Process Technol 136:158–165
22. Gillner A, Holtkamp J, Hartmann C, Olowinsky A, Gedicke J, Klages K, Bosse L, Bayer A (2005) Laser applications in microtechnology. J Mater Process Technol 167:494–498
23. Fausett L (1994) Fundamentals of neural networks: architectures, algorithms and applications. Prentice-Hall, New York